International Journal of Mass Spectrometry 294 (2010) 33–39

Contents lists available at ScienceDirect

International Journal of Mass Spectrometry

journal homepage: www.elsevier.com/locate/ijms

An optimised compact electron impact ion storage source for a time-of-flight mass spectrometer

Dominic Abplanalp*, Peter Wurz, Liliane Huber, Ingo Leya

Physikalisches Institut, Universität Bern, Sidlerstrasse 5, 3012 Bern, Switzerland

ARTICLE INFO

Article history:
Received 5 August 2009
Received in revised form 14 April 2010
Accepted 3 May 2010
Available online 10 May 2010

Keywords:
Electron impact ionisation
TOF-MS
Ion storage source
Electrostatic field separation
Space research

ABSTRACT

In the ion source of an ion trap time-of-flight (TOF)-mass spectrometer, an effective electrostatic field separation of the region of ion generation and ion acceleration, which have different electric field strengths, is necessary for optimal operation. At the same time, the electrostatic field separation has to have a high transmission for ions, permitting for a high sensitivity of the mass spectrometer. Usually, a single mesh is used for such an application. In our case of a compact yet high-performance system, the field separation requirements are too tight for using only a single mesh. We systematically performed ion-optical simulations, which showed that only a double grid configuration promises satisfying results. The modifications of the instrument, based on the simulations, increased the performance significantly by reducing the baseline and improving the storage of the ions; the dynamic range of the modified spectrometer after the improvements covered – in a 1 min record time – about six orders of magnitude. Systematic studies performed using the laboratory instrument confirm the results of the simulations.

1. Introduction

One of the main advantages of time-of-flight (TOF) mass spectrometers is their ability to analyze all gas species simultaneously [1]. We have designed and built a new time-of-flight mass spectrometer able to measure neutral gases (see Fig. 1). The instrument has a high sensitivity (partial pressures of 10^{-14} mbar are detectable in a 60 s measurement) and a mass resolution of $m/\Delta m$ (FWHM) > 1000 [2]. Since a later version of this instrument should fulfill the requirements for space applications, e.g., to investigate the composition of the Martian atmosphere, there is a need for a very compact size.

For this mass spectrometer we have developed a small electron impact storage source (see Figs. 2 and 3). Unlike earlier realizations of a storage source using a grid in the centre of the ionisation region to create a local electrostatic depression to store the ions [3], our new version uses instead only the potential depression resulting from the space charge of the electron beam in the ionisation region. Our source is rotationally symmetric with respect to the principal ion-optical axis, i.e., along the direction of ion extraction. From the cathode electrons are continuously released and are accelerated towards the centre of the ion source by a ring electrode. The energy of the electrons is given by the potential difference between the cathode and the ring electrode, thus changing one or both potentials can vary the energy. The electrons move perpendicular to the ion-optical axis and, on their way to the electron trap, ionise the neutral atoms. The thus continuously produced ions are stored for a certain time between the backplane and the extraction grid and, by applying a negative potential on the extraction grid, are extracted in a short burst into the TOF section. The further ion acceleration is such that short ion packets are formed at the first time focus shortly after the exit of the ion source, from where the ion mirror images these ion packets onto the detector plane (second time focus).

In TOF instruments the storage of ions significantly increases the efficiency of the spectrometer, which otherwise would be low because of the duty cycle of the ion extraction. Without storage only those atoms that are ionised at the time of the extraction pulse are extracted into the TOF system and measured in the detector, all other ions are lost. Assuming an extraction pulse length of about 100 ns and a pulse frequency of 1 kHz gives that only 1 out of 10^4 atoms are analyzed. Consequently, the storage of ions is of special importance if only a small number of atoms are available for analysis. Every ion that is not stored is lost. Even worse, almost every ion that is not stored but nevertheless reaches the TOF section also causes a signal in the detector. However, since its arrival is not correlated with the start pulse in the ion source, the timing of its arrival is not correlated to its mass. Not only are these kind of ions lost for successive measurements, but also they generate a background in the mass spectra by increasing the baseline and decreasing the sensitivity. We call this phenomenon a leaking storage source.

* Corresponding author. Tel.: +41 031 631 44 57; fax: +41 031 631 44 05.
E-mail addresses: dominic.abplanalp@space.unibe.ch, abplanalp@space.unibe.ch (D. Abplanalp).

1387-3806/$ – see front matter © 2010 Elsevier B.V. All rights reserved.
doi:10.1016/j.ijms.2010.05.001

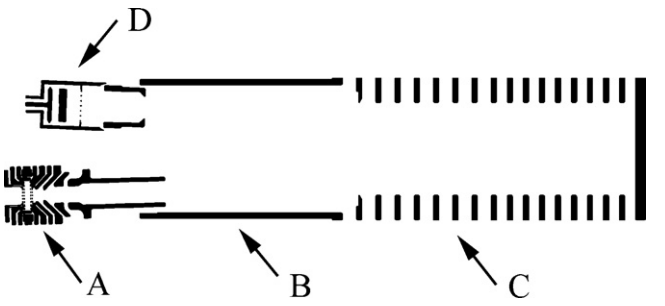

Fig. 1. Schematic overview of the mass spectrometer with the ion source and acceleration electrodes (A), the drift tube (B), the reflectron (C), and the detector (D).

In order to store the ions, the ionisation region has to be almost field-free during the storage phase, otherwise the ions would be accelerated and would leave the source. This nearly field-free region in the source is modified by the space charge of the electron beam and by the stored ions. The space charge of the electrons holds the ions back, but only in two dimensions; not in the direction of the electron flight path. In the direction of the electron flight path, the ions can be stored by carefully adjusted electrode potentials. It is obvious that only those ions whose kinetic energy is smaller than the space charge potential will be stored and after a certain time the space charge of the stored ions completely cancels the space charge of the electron cloud, i.e., the trap is filled. Before this charge cancellation point is reached, an electrical pulse with a very fast rise time is applied to the extraction grid to produce an electrical field in the ionisation region and to accelerate the ions into the TOF section.

The main problem in this set-up is to separate the static electric fields of the acceleration region from the source region, which should be nearly field-free during ion storage. In other words, the difficulty is to separate a nearly field-free region (source) from a region with a strong electrostatic field (analyzer). As an additional requirement, this boundary has to be highly permeable for the ions during ion extraction but also has to have a sharp potential gradient between acceleration and ionisation region. Normally, a fine metallic mesh is used to separate the two regions, a method which is also very often applied in TOF-mass spectrometry [3–5], with a better separation for smaller mesh sizes. However, a small mesh size reduces the transmission of the ions from the source to the analyzer, which is a limiting factor for measurements of small gas amounts. Consequently, in our first prototype version of the mass spectrometer we used only a single extraction grid with a geometric transmission of 90%. The disadvantage of a single grid is a relatively strong field penetration through the mesh, depending on the potential differences and the characteristics of the mesh. We tried to compensate the field penetration in the ionisation region by adjusting some voltages, in particular the potentials of the backplane and the extraction grid, but first measurements indicated a significantly leaking storage source. After having realized that adjusting the potentials is not good enough we performed a series of simulations using SIMION [6], refining the modeling of the grids and the field penetration. The results of these simulations and the experimental improvements for the ion source are the main topics of this publication.

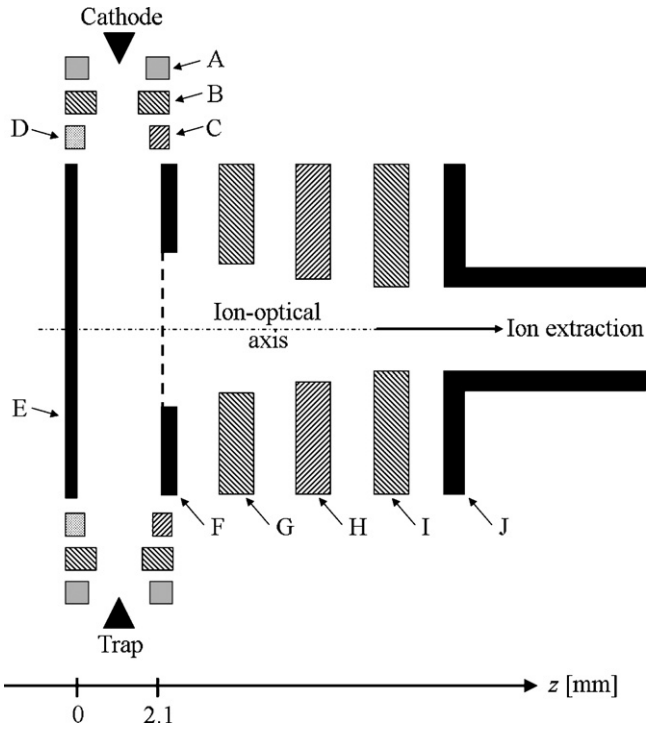

Fig. 2. Simplified electrode configuration of the ion storage source with the cathode (−70 V), the electron trap (+5 V), A) electron repeller (−65 V), B) ground (0 V), C) ion repeller 1 (+2 V), D) ion repeller 2 (+2 V), E) backplane (0 V), F) extraction grid (0 V/−400 V), G) ion lens 1 (−1.3 kV), H) ion lens 2 (−2.0 kV), I) ion lens 3 (−4.2 kV), J) drift tube (−1.9 kV). All potentials are relative to ground.

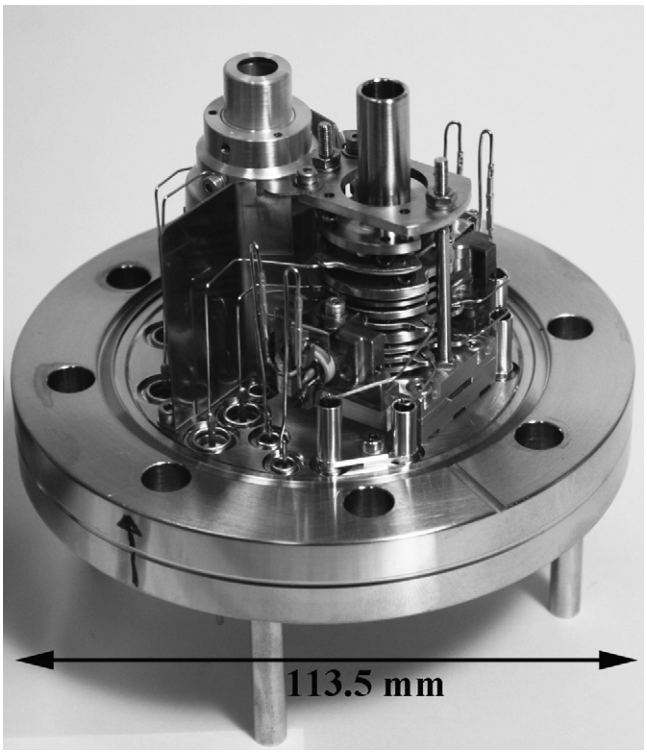

Fig. 3. The ion storage source and the detector (background) are directly mounted on a CF-63 vacuum flange with all corresponding electrical feed-throughs. At the top of the ion source, several acceleration electrodes and the first part of the drift tube are visible. Sapphire balls with different diameters are used as isolators between the electrodes.

2. Description of the mass spectrometer

The mass spectrometer consists of five major parts: an electron impact storage ion source (Fig. 1A), an acceleration region (Fig. 1A), a field-free drift region (Fig. 1B), a gridless reflectron (Fig. 1C), and a detector (Fig. 1D). The overall length is 290 mm, the inner diameter is 70 mm and thus the volume of the total system is less than 1.3 L. The effective ion flight path is about 0.5 m. The reflectron is placed in the tube on the symmetry axis together with its drift tube, and

the ion source and the detector form a narrow V-geometry with the reflectron in its apex. The flight time of a single positively charged ^{132}Xe ion is about 10 μs. The mass spectrometer and its experimental testing on a long duration balloon flight in the stratosphere are described in detail by Abplanalp et al. [7] and Wieser et al. [8].

The ion source is on a two-field acceleration electron impact ion source first invented by Wiley and McLaren [9], but realizing the second acceleration stage without any additional grids. The impact electrons have a typical energy of 70 eV and the electron emission is about 200 μA. The ionisation region is a small gap defined by a backplane (Fig. 2E) on one side and an extraction grid (Fig. 2F) on the other side. The electron beam is guided into this gap using several electron repellers (Fig. 2A and B). Some ion repellers (Fig. 2C and D) are placed along the electron beam axis to allow for ion confinement also in this direction. The gap between the backplane and the extraction grid is 2.1 mm and the grid has a diameter of 4.5 mm. In front of the extraction grid there are electrodes at static potentials for accelerating and focusing the ions leaving the trap region (Fig. 2G–I). The distance of the nearest acceleration electrode from the extraction grid is 1.1 mm, resulting in an electrical field of 1.2 kV/mm in front of the extraction grid. Considering this electrical field, it is obvious that our goal of a field-free region between the backplane and the extraction grid is very challenging.

Most of the time, the potentials in the source are set to store the ions, i.e., no positively charged particle can escape from the source into the analyzer section. With a characteristic frequency of 1 to 10 kHz, a negative pulse with a very fast rise time is applied to the extraction grid in order to produce an electrical field in the ionisation region. This electrical field extracts the ions into the TOF section. The measured rise time of the applied extraction pulse is 3.3 ns (10–90%) and the extraction potential is applied for a period of 1.5 μs, followed by a relatively slow increase of the potential back to zero during about 0.5 μs. At the end of this slow increase, the potential of the grid is fixed again in the storage mode for, depending on the used pulse frequencies, between 100 μs and 1 ms, depending on the frequency of the extraction pulse.

The acceleration region, which consists of three electrodes, is followed by a drift tube, and the reflectron. The latter is a custom-made grid-free two-stage ion mirror with an electrostatic lens at the entrance. The set-up is similar to the RTOF instrument [4,5] but significantly smaller. The inner diameter of our reflectron is 28.8 mm and its total length is 87 mm. The electric field in the mirror is made using altogether 17 ring electrodes, which also allow a second order time focusing of the ions. The second order time focusing of ion reflectron was invented in the early 1970s by Mamyrin et al. [10]. The detector is a custom-made using two microchannel plates in a chevron configuration having an active area of 50 mm^2. The anode is designed for a correct impedance match to the 50 Ω signal line to ensure clean pulse shapes and no ringing. The acquisition and processing of the detector signals are via an analogue-to-digital converter (ADC) from Acqiris (AP240, 8-bit signal analyzer), which is triggered by the extraction pulse.

3. Grid simulations

For our first prototype of the mass spectrometer we used only a single grid to maximize the ion transmission. It soon became clear that the set-up using only a single grid is not sufficient to separate the potentials of the ionisation and the acceleration region. Due to the partial penetration of electrical fields from the acceleration into the ionisation region, ions continuously leaked out of the source into the mass analyzer system and thus significantly increased the baseline of the spectra. We therefore performed systematic ion-optical simulations of the grids using the SIMION software system. In particular we varied the characteristics of the mesh in order to find the best solution for our special application.

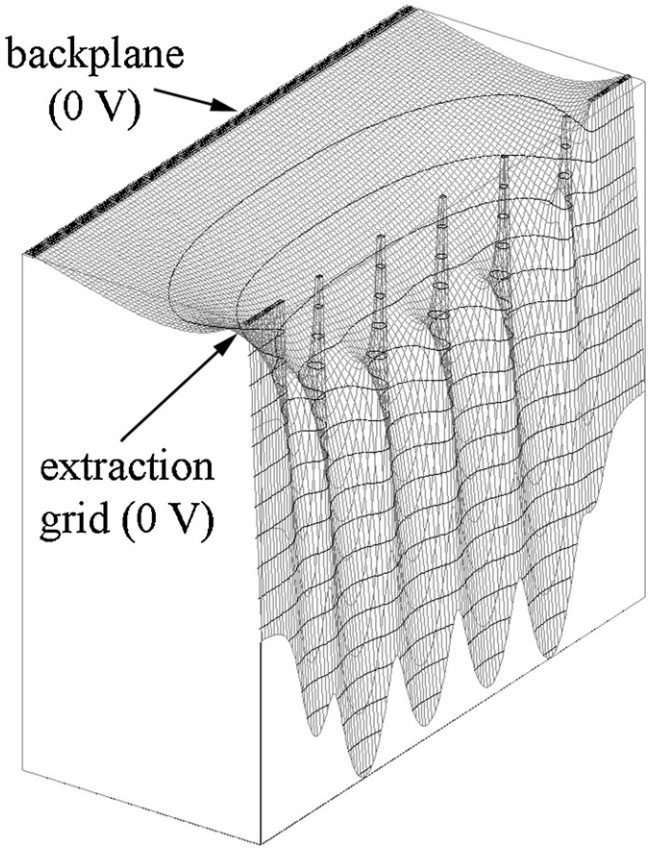

Fig. 4. Original single grid with a wire diameter d_w of 0.043 mm and a space between the wires d_g of 0.803 mm. The plot is a 3-D view of the electrostatic potential in the middle of the source. The potentials of the backplane and the extraction grid are set to 0 V. The potentials of the lenses are the same as shown in the caption of Fig. 2. The plotted lines are the 10 V-equipotential lines, thus in the middle of the source the electrostatic field is on average about 28 V/mm.

3.1. Single grids

The original grid was a copper Buckbee-Mears grid (MC-8), wire diameter d_w of 0.043 mm, space between the wires d_g of 0.803 mm (centre-to-centre). As expected and shown in Fig. 4, the field penetration is significant as indicated by the SIMION model calculations. In addition, the leaking electrical field also produces field inhomogeneities in the ionisation region.

As can be seen in Fig. 4, the penetration of the electrostatic field from the acceleration into the ionisation region is strong and cannot be compensated for by adjusting grid or backplane potentials. The modeling also demonstrates that some of the electrons are deflected towards the backplane and therefore never pass through the gap to reach the electron trap, which significantly compromises the ionisation efficiency. The few ions produced in the ion source are basically from near the electron entrance into the gap and the most of them are not stored but are immediately lost into the TOF section. The results of the simulation are consistent with the experimental observation of a leaking storage source.

We also performed simulations of a pulsed first acceleration electrode (Fig. 2G). In this simulation, the potential of lens 1 is set to 0 V during the storage mode and is set to −1.3 kV in the extraction mode. The new set-up decreases the electrostatic field strength in front of the extraction grid during the storage mode but the field penetration through the mesh is still too high. Additionally, the fast change of such high voltages would generate a lot of electromagnetic interferences, which would compromise the detector performance.

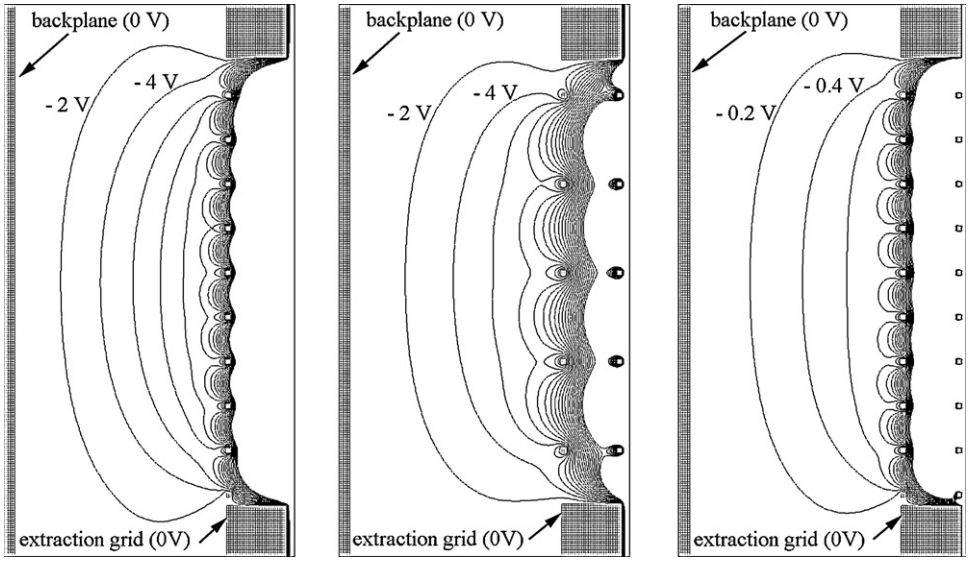

Fig. 5. Results of three different SIMION simulations. *Left panel*: Fine single grid with a wire thickness of 0.04 mm and a mesh size of 0.4 mm. The 2 V-equipotential lines are plotted only in the relevant area of the source. *Middle panel*: Original mesh (wire thickness = 0.04 mm, wire distance = 0.8 mm) in a double grid configuration. The distance of the two grids is 0.4 mm. The 2 V-equipotential lines are plotted again only in the relevant area of the source. *Right panel*: Fine mesh (wire thickness = 0.04 mm, wire distance = 0.4 mm) in a double grid configuration. The distance of the two grids is 0.4 mm. The 0.2 V-equipotential lines are plotted again only in the relevant area of the source. All potentials of the electrodes are the same as given in the caption to Fig. 2.

The left panel of Fig. 5 shows the results of a simulation using a finer single mesh, still with a wire diameter of d_w = 0.04 mm but now with a mesh width of d_g = 0.4 mm (instead of 0.8 mm). The electrostatic field in the middle of the storage source averages to 6 V/mm (compared to 28 V/mm). As expected, although using a finer mesh reduces the field penetrations into the storage source, the reduction is far from sufficient. A possible solution could be using even finer meshes. However, this would not only reduce the transmission of the ions through the mesh, for finer meshes not only d_g but also d_w has to be smaller, which makes their manufacture increasingly more difficult. Moreover, the manipulation and installation of such fine structures becomes extremely difficult. Consequently, using much finer meshes is not realistic and would significantly compromise the performance of the spectrometer.

3.2. Double grids

Another possibility for electrostatic field separations are double grids, i.e., two identical parallel meshes at the same potential, whereas the wires of the first grid have to be perfectly aligned with the wires of the second grid. The middle panel of Fig. 5 shows a double grid configuration with d_w = 0.04 mm and d_g = 0.8 mm; the two grid planes are separated by a distance of 0.4 mm. The electrostatic field in the middle of the storage source averages again to 6 V/mm, i.e., close to the value obtained using a fine single grid with d_w = 0.04 mm and d_g = 0.4 mm (left panel of Fig. 5). The right panel of Fig. 5 shows the results of the simulation using a double grid with d_w = 0.04 mm and d_g = 0.4 mm, with the distance between the two grids again 0.4 mm. In this simulation, the electrostatic field in the middle of the storage source averages at 0.45 V/mm, which is within acceptable limits and which can at least partly be compensated for by a slight adjustment of the backplane and extraction grid potentials.

4. Results

The SIMION simulations of the different grids clearly demonstrate that the original set-up with only one grid is not sufficient to separate the source from the acceleration region. Using the same grid in a double grid configuration significantly reduces the field penetration. A similar reduction of the field penetration is achieved using a single grid with a finer mesh. However, neither version is satisfying. The best results are obtained using a double grid with a fine mesh. The mesh chosen by us efficiently separates both regions (source–accelerator) but is still stable enough for handling (see Figs. 6 and 7).

The SIMION simulation of the ion trajectories indicates that the transmission of the ions in the double grid configuration (fine mesh) is only slightly lower than by using the original single grid. The simulations were performed assuming 3-D Gaussian-distributed starting points for the ions with the centre of the distribution in the middle of the ion source for all three spatial directions. The standard deviation of the distribution was chosen such that 99% of the ions started between the backplane and the extraction grid (in *z*-direction) and between −2.5 mm and +2.5 mm (in *x*-

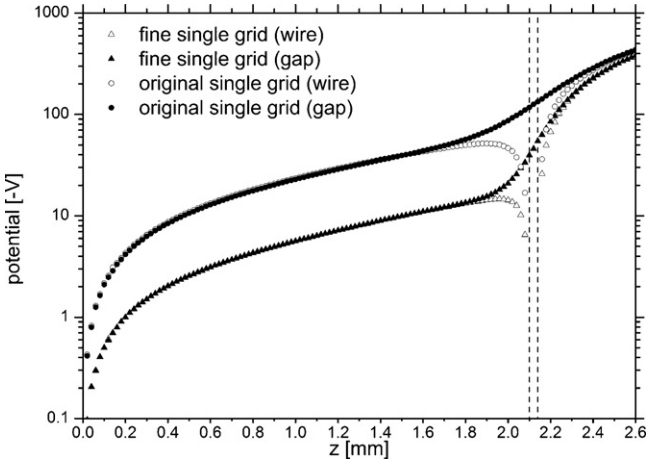

Fig. 6. The characteristics of the electrostatic potentials along the ion-optical axis in the single grid source in storage mode. The plot corresponds to the set-up of Fig. 4 (original grid) and the left panel of Fig. 5 (fine grid). Inside of the source, at a distance of about d_g from the extraction grid, the difference of the potential characteristics along a wire cross and a wire gap are negligible. The dashed lines at 2.1 mm and 2.14 mm indicate the front and backside of the single grid, respectively.

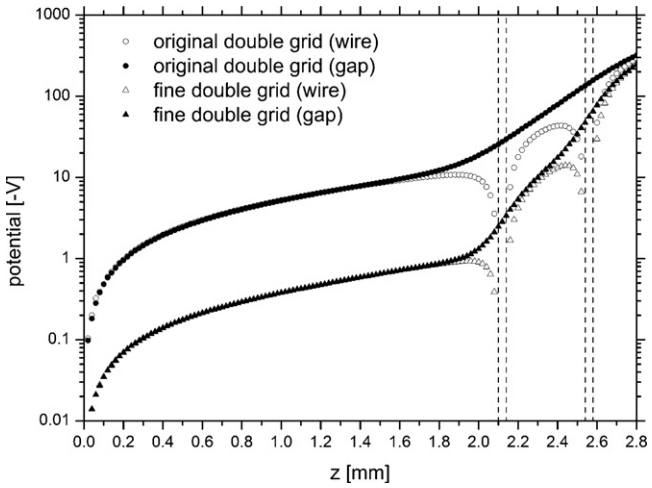

Fig. 7. The characteristics of the electrostatic potentials along the ion-optical axis in the source with double grids in storage mode. The plot corresponds to the set-up of the middle panel of Fig. 5 (original grid) and the right panel of Fig. 5 (fine grid). Inside of the source, after a distance of about d_g away from the extraction grid, the difference of the potential characteristics along a wire cross and a wire gap can be neglected. The dashed lines at 2.1 and 2.14 mm and at 2.54 and 2.58 mm indicate the front and backsides of the two grids, respectively.

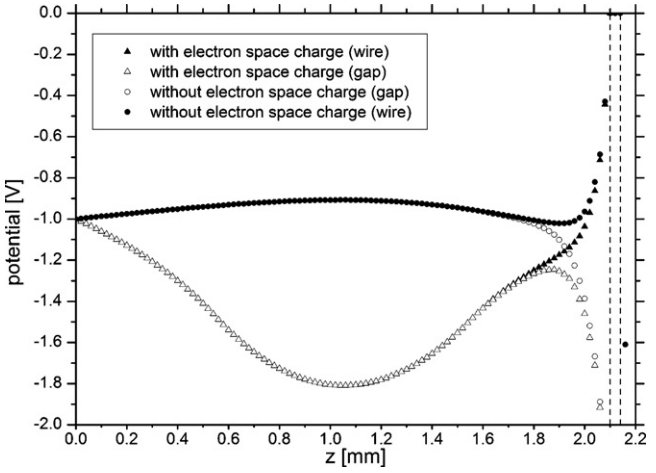

Fig. 8. The potential characteristics of the ion source including the space charge of the electron cloud. The set-up is the same as in the right panel of Fig. 5, but with a backplane potential of −1 V.

and y-direction). The starting directions of the ions were uniform distributed in 3-D space and the starting energy was uniformly distributed in the range 0.06–0.2 eV. In each simulation we followed the trajectories of 10^4 ions. For the original single grid we obtained an ion-optical transmission of 71%; for the fine single grid we obtained a transmission of 62%. For the original mesh in a double grid configuration the transmission was also 62% and for the fine double grid the simulation gives a transmission of 51%. However, the slightly reduced transmission of the fine double grid is more than compensated for by better ion storage and significantly reduced background. The field penetration modeled by us is in the same range as described by Read et al. [11]; the deviations between both approaches is most likely due to the different wire and electrode geometries used in both set-ups. Note that the field distortions near the grid can act as an electrostatic lens and can therefore change the direction of the passing ions, which can reduce the transmission and the mass resolution of the mass spectrometer (see Bergmann et al. [12]). We did not checked for such effects because we consider them as only very minor for our instrument since the TOF path length is short in our instrument.

Fig. 8 shows the potential distribution of the double grid configuration, with the backplane at −1 V and the extraction grid at ground potential. For calculating the electrostatic potentials the space charge of the electron beam is also considered. The space charge of the electron cloud is estimated according to

$$\phi_{out}(R_e \le r \le R_a) = \frac{I_{el}}{2 \cdot \pi \cdot \varepsilon_0} \cdot \sqrt{\frac{m_e}{2 \cdot K_e}} \cdot \ln\left(\frac{r}{R_a}\right) \quad (1)$$

and

$$\phi_{in}(0 \le r \le R_e) = \frac{I_{el}}{4 \cdot \pi \cdot \varepsilon_0} \cdot \sqrt{\frac{m_e}{2 \cdot K_e}} \cdot \left(2 \cdot \ln\left(\frac{R_e}{R_a}\right) + \frac{r^2}{R_e^2} - 1\right) \quad (2)$$

assuming a cylindrical homogenous electron beam with a radius R_e of 0.5 mm and with the electron emission I_{el} = 0.2 mA, the electron energy K_e = 70 eV, m_e the electron mass (in kg), e the charge of the electron (in C), and R_a as half the distance between the backplane and the extraction grid (1.05 mm). Therefore the maximum space charge depression is about 0.9 V at r = 0 (in the middle of the source) [13].

Motivated by these simulations, we decided to build a new extraction grid configuration for our instrument, using two identical parallel meshes at a distance of 0.4 mm, a wire thickness d_w of 0.04 mm, and a mesh size of d_g = 0.4 mm (see Fig. 9). As can been seen by comparing Fig. 10 (original set-up) and Fig. 11 (new double grid configuration) the results of our first measurements with the new grid configuration were satisfying; the baseline of the spectrum has been significantly reduced, the dynamic range has been increased by more than five orders of magnitude, and the efficiency to detect small mass ions has been increased. The new grid configuration allows recording mass spectra (analysis time 66 s) with a dynamic range of about six orders of magnitude. Note that we were able to further improve the signal-to-noise ratio and therefore to further increase the dynamic range of the instrument by sophisticated adjustments of the source potentials and by adding a well adapted front end electronics.

Fig. 9. The extraction electrode with the new fine double grid configuration. The diameter of the grids are 4.5 mm, the distance between the two grids is 0.4 mm.

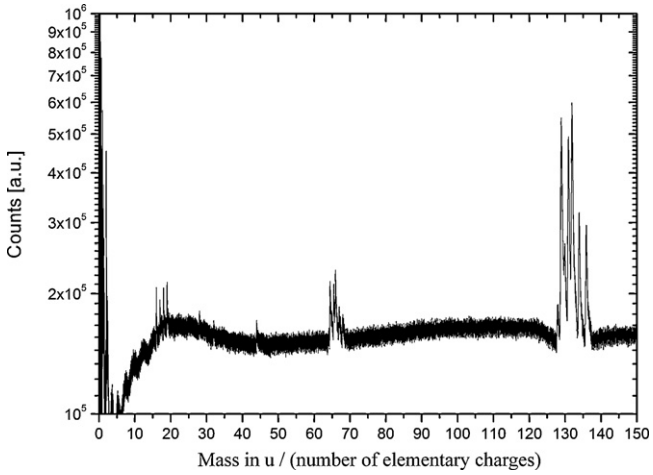

Fig. 10. Typical mass spectrum of Xenon using the original single grid configuration (record time 66 s). The baseline is relatively high and therefore the small mass peaks are not visible. The dynamic range is strongly limited.

If the leaking of the electrical field from the acceleration into the source region is small enough the potential wall by the electrons becomes deep enough and storing of ions becomes possible (see Fig. 8). One possibility to verify the storage characteristics of the ion source is to study the height of the signals as a function of the electron current. Fig. 12 shows the results of the theoretical calculations [14] in the interesting range of electron currents from 1 to 20 μA. The calculations predict that in these range the signals should be proportional to $I_{el}^{2.75}$. Comparing laboratory measurements with our predictions indicates that only about 10–12% of the electrons emitted from the cathode pass through the gap to reach the trap and produce the potential wall (with these specific potential settings), the rest of the electrons is deflected somewhere. Consequently, only about 10–12% of the emitted electrons are effective usable for the ionisation of neutrals and for generating a space charge potential to store the produced ions. Fig. 12 shows the number of extracted $^{14}N_2^+$ ions per 10^4 pulses as a function of the effective usable electron current, which is about 10–12% of the total current. The agreement of the experimental data with the theoretical calculations is good.

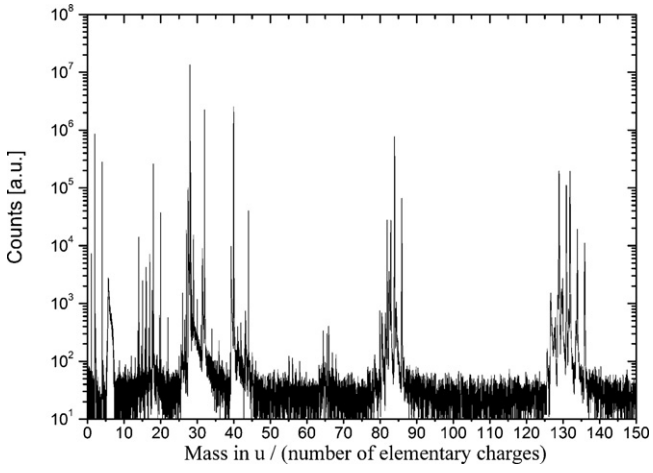

Fig. 11. Typical mass spectrum of a noble gas mixture with the new fine double grid configuration (record time 66 s). The baseline is distinctively lower and therefore small mass peaks are also visible. The dynamic range covers more than five orders of magnitude.

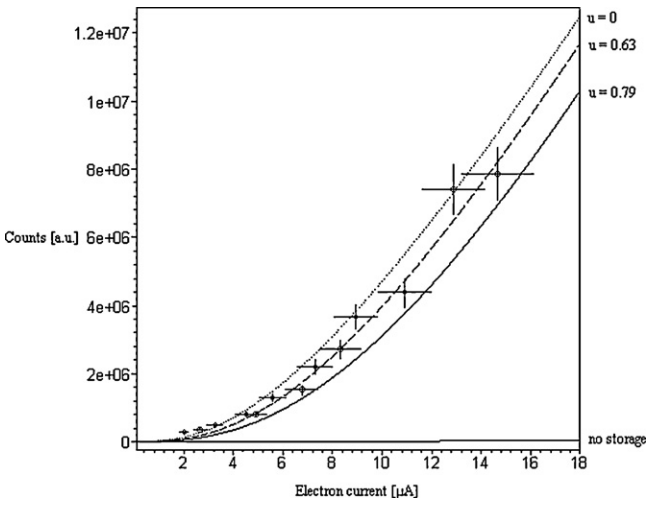

Fig. 12. Number of extracted $^{14}N_2^+$ ions per 10^4 pulses as a function of the electron current. The lines represent the theoretical calculations for different ion production locations (u is in the range of [0,1] with $u = 0$ the middle of the source and $u = 1$ the boundary of the source). In addition, the calculated number of extracted ions in the non-storage mode is plotted (line at the bottom of the plot). The symbols are the experimental data of $^{14}N_2^+$ mass peaks with 10%-error bars.

5. Conclusions

A proper electrostatic field separation of two or more regions by preserving a high ion-optical transmission is important for various practical applications. Our ion-optical SIMION simulations and the bad performance of our first prototype spectrometer, no storage and low dynamic range, clearly demonstrated that a single grid not always guarantees a sufficient separation of the electrical fields. Using double grids is not really a new approach, but our work clearly demonstrates the significant improvement for separating different field regions with only minor losses of ion transmission. We performed a variety of simulations to find the best solution for our application. By modifying the mass spectrometer according to the modeling we were able to significantly improve the performance of the ion source, i.e., storage and high dynamic range.

References

[1] R.J. Cotter, Time-of-Flight Mass Spectrometry, American Chemical Society, Washington, 1997.
[2] D. Abplanalp, Master's Thesis, Kleinstmassenspektrometer für planetologische Untersuchungen, University of Bern, Switzerland, 2005.
[3] R. Grix, U. Grüner, G. Li, H. Stroh, H. Wollnik, An electron impact storage ion source for time-of-flight mass spectrometers, Int. J. Mass Spectrom. Ion Process. 93 (1989) 323–330.
[4] S. Scherer, K. Altwegg, H. Balsiger, J. Fischer, A. Jäckel, A. Korth, M. Mildner, D. Piazza, H. Rème, P. Wurz, A novel principle for an ion mirror design in time-of-flight mass spectrometry, Int. J. Mass Spectrom. 251 (2006) 73–81.
[5] H. Balsiger, K. Altwegg, P. Bochsler, P. Eberhardt, J. Fischer, S. Graf, A. Jäckel, E. Kopp, U. Langer, M. Mildner, J. Müller, T. Riesen, M. Rubin, S. Scherer, P. Wurz, S. Wüthrich, E. Arijs, S. Delanoye, J. De Keyser, E. Neefs, D. Nevejans, H. Rème, C. Aoustin, C. Mazelle, J.-L. Médale, J.A. Sauvaud, J.-J. Berthelier, J.-L. Bertaux, L. Duvet, J.-M. Illiano, S.A. Fuselier, A.G. Ghielmetti, T. Magoncelli, E.G. Shelley, A. Korth, K. Heerlein, H. Lauche, S. Livi, A. Loose, U. Mall, B. Wilken, F. Gliem, B. Fiethe, T.I. Gombosi, B. Block, G.R. Carignan, L.A. Fisk, J.H. Waite, D.T. Young, H. Wollnik, ROSINA - Rosetta orbiter spectrometer for ion and neutral analysis, Space Sci. Rev. 128 (2007) 745–801.
[6] D.A. Dahl, SIMION3D Version 7.0, User's Manual, Idaho National Engineering and Environmental Laboratory, Ringoes, NY, 2000.
[7] D. Abplanalp, P. Wurz, L. Huber, I. Leya, E. Kopp, U. Rohner, M. Wieser, L. Kalla, S. Barabash, A neutral gas mass spectrometer to measure the chemical composition of the stratosphere, Adv. Space Res. 44 (2009) 870–878.
[8] M. Wieser, L. Kalla, S. Barabash, T. Hedqvist, S. Kemi, O. Widell, D. Abplanalp, P. Wurz, The Mars environment analogue platform long duration balloon flight, Adv. Space Res. 44 (2009) 308–312.

[9] W.C. Wiley, I.H. McLaren, Time-of-flight mass spectrometer with improved resolution, Rev. Sci. Instrum. 26 (1955) 1150–1157.
[10] B.A. Mamyrin, V.I. Karataev, D.V. Shmikk, V.A. Zagulin, The mass-reflectron, a new nonmagnetic time-of-flight mass spectrometer with high resolution, Sov. Phys. JEPT 37 (1973) 45–48.
[11] F.H. Read, N.J. Bowring, P.D. Bullivant, R.R.A. Ward, Penetration of electrostatic fields and potentials through meshes, grids, or gauzes, Rev. Sci. Instrum. 69 (1998) 2000–2006.
[12] T. Bergmann, T.P. Martin, H. Schaber, High-resolution time-of-flight mass spectrometers: Part I. Effects of field distortions in the vicinity of wire meshes, Rev. Sci. Instrum. 60 (1989) 347–349.
[13] S. Scherer, Design of a high-performance Reflectron time-of-flight mass spectrometer for space applications, PhD Thesis, University of Bern, Switzerland, 1999.
[14] D. Abplanalp, Development of a sensitive TOF-mass spectrometer for space research, PhD Thesis, University of Bern, Switzerland, 2009.